

LETTER TO THE EDITOR

Dynamical formation of Gaia BH3 in the progenitor globular cluster of the ED-2 stream

Daniel Marín Pina¹, Sara Rastello¹, Mark Gieles^{1,2}, Kyle Kremer³, Laura Fitzgerald¹, Bruno Rando¹

¹ Departament de Física Quàntica i Astrofísica, Institut de Ciències del Cosmos, Universitat de Barcelona, Martí i Franquès 1, E-08028 Barcelona, Spain

e-mail: danielmarin@icc.ub.edu

² ICREA, Pg. Lluís Companys 23, E08010 Barcelona, Spain

³ TAPIR, California Institute of Technology, Pasadena, CA 91125, USA

Received XX; accepted XX

ABSTRACT

Context. The star-black hole (S-BH) binary discovered by the *Gaia* Collaboration – *Gaia* BH3 – is chemically and kinematically associated with the metal-poor ED-2 stream in the Milky Way halo.

Aims. We explore the possibility that *Gaia* BH3 was assembled dynamically in the progenitor globular cluster (GC) of the ED-2 stream.

Methods. We use a public suite of star-by-star dynamical Monte Carlo models by Kremer et al. (2020) to identify S-BH binaries in GCs with different initial masses and (half-mass) radii.

Results. We show that a likely progenitor of the ED-2 stream was a relatively low-mass ($\lesssim 10^5 M_\odot$) GC with an initial half-mass radius of 2 – 4 pc. Such a GC can dynamically retain a large fraction of its BH population and dissolve on the orbit of ED-2. From the suite of models we find that GCs produce $\sim 3 - 30$ S-BH binaries, approximately independent of initial GC mass and inversely correlated with initial cluster radius. Scaling the results to the Milky Way GC population, we find that $\sim 75\%$ of the S-BH binaries formed in GCs are ejected from their host GC in the early phases of evolution ($\lesssim 1$ Gyr); these are expected to no longer be close to the stream. The $\sim 25\%$ of S-BH binaries retained until dissolution are expected to form part of streams, such that for an initial mass of the progenitor of ED-2 of a few $10^4 M_\odot$, we expect $\sim 2 - 3$ S-BH to end up in the stream. GC models with metallicities similar to *Gaia* BH3 ($\lesssim 1\%$ solar) include S-BH binaries with similar BH masses ($\gtrsim 30 M_\odot$), orbital periods, and eccentricities.

Conclusions. We predict the Galactic halo contains of order 10^5 S-BH binaries that formed dynamically in GCs, a fraction of which may readily be detected in *Gaia* DR4. The detection of these sources provides valuable tests of BH dynamics in clusters and the possible role in formation of gravitational wave sources.

Key words. Stars: black holes – Stars: Population II – Galaxy: kinematics and dynamics – Galaxy: halo-globular clusters

1. Introduction

The discovery of a star-black hole (S-BH) binary by the *Gaia* collaboration (Gaia Collaboration 2024) – *Gaia* BH3 – constitutes another glimpse into the population of dormant BHs. *Gaia* BH3 is composed of a $33 M_\odot$ BH with a $0.76 M_\odot$ star. The star is a metal-poor giant, with metallicity $[\text{Fe}/\text{H}] \approx -2.6$. The binary has an eccentricity of $e \approx 0.73$, and a wide orbit with period $P \approx 4200$ d. *Gaia* BH3 is on a halo orbit, similar to the debris of the Sequoia accretion event (Gaia Collaboration 2024).

The previously discovered *Gaia* BH1 (El-Badry et al. 2023b) is a binary with a Sun-like star orbiting a BH with a mass $m_{\text{BH}} \approx 10 M_\odot$, an eccentricity $e = 0.45$, and a period of $P \approx 186$ d. *Gaia* BH2 (El-Badry et al. 2023a) is a binary with a red giant orbiting a $m_{\text{BH}} \approx 9 M_\odot$ BH, with an eccentricity $e \approx 0.5$, and a relatively long period of $P \approx 1280$ d. Their metallicities ($[\text{Fe}/\text{H}] \approx -0.2$) and their inferred orbits in the Galactic plane point towards a formation in a young stellar population, possibly an open cluster (Rastello et al. 2023; Di Carlo et al. 2024; Tanikawa et al. 2024; Arca Sedda et al. 2024) or an isolated stellar binary (Kotko et al. 2024).

The association of *Gaia* BH3 with the stellar halo calls for another formation scenario. Under the assumption that the un-

seen companion is a single BH¹, Gaia Collaboration (2024) argue that formation of *Gaia* BH3 in isolation is unlikely. The star does not present strong chemical peculiarities, indicating a lack of pollution by the BH progenitor in its evolved stage. This makes a dynamical formation scenario, where the system is assembled after the BH progenitor has exploded as a supernova, more plausible. Its orbit in the Galactic halo and low metallicity suggest that *Gaia* BH3 formed in a globular cluster (GC).

Balbinot et al. (2024) show that *Gaia* BH3 is both chemically and kinematically associated with the ED-2 stream (Dodd et al. 2023). The progenitor of the ED-2 stream was most likely a GC, given its low velocity dispersion (Balbinot et al. 2023) and the absence of an $[\text{Fe}/\text{H}]$ spread (< 0.04 dex, Balbinot et al. 2024). These authors also find a negligible spread in Na and Al, suggesting an initial cluster mass $\lesssim 4 \times 10^4 M_\odot$. The maximum initial mass of a cluster with BHs that can dissolve in 13 Gyr on the orbit of ED-2 is $\sim 9 \times 10^4 M_\odot$ (Gieles & Gnedin 2023).

So far, only two (possibly three) detached stellar-mass BH binary candidates have been found in GCs (in NGC 3201,

¹ The available data can not rule out that the unseen object is a binary BH (BBH).

Giesers et al. 2018, 2019)². Only line-of-sight velocities are available for these binaries, providing a minimum BH mass of $\gtrsim 5 M_{\odot}$. Kremer et al. (2018b) showed that these binaries were likely formed and shaped via dynamical exchange interactions. Evidence for massive BHs ($\gtrsim 30 M_{\odot}$) in a (dissolved) GC is critical to understand the contribution of dynamically-produced BBHs to the growing sample of gravitational wave sources (e.g., Portegies Zwart & McMillan 2000; Rodriguez et al. 2016; Askar et al. 2017; Antonini et al. 2023).

In this Letter we show that *Gaia* BH3 could have formed dynamically in the progenitor GC of the ED-2 stream. In Sec. 2 we describe the dynamical models of GCs that we use to search for S-BH binaries. In Sect. 3 we present the properties of S-BH in the models and the implications are discussed in Sect. 4. A discussion and conclusions are presented in Sect. 5 and 6, respectively.

2. Methods

We use the suite of GC simulations run with the CLUSTER MONTE CARLO (CMC) code. CMC is a Hénon-type Monte Carlo code for the long term evolution of collisional stellar systems (Rodriguez et al. 2022, and references therein). The integration is done on a star-by-star basis, following gravitational interactions, the internal evolution of stars and binary stars, strong few-body interactions and dynamical ejections (Weatherford et al. 2023). Further details on the code can be found in Rodriguez et al. (2022).

For this work, we use the set of 148 CMC models presented in Kremer et al. (2020). This catalog is meant to sample the relevant parameter space of local-universe GCs varying the following initial conditions: the number of stars N , virial radius r_v^3 , metallicity Z , and Galactocentric distance R_G . The choice of values for the above parameters is $N \in [2, 4, 8, 16] \times 10^5$, $r_v \in [0.5, 1, 2, 4]$ pc, $Z \in [0.0002, 0.002, 0.02]$, and $R_G \in [2, 8, 20]$ kpc, which account for 144 models, plus four extra models with $N = 3.2 \times 10^6$, $R_G = 20$ kpc, $Z \in [0.0002, 0.02]$, and $r_v \in [1, 2]$ pc.

We first look at the raw results of all S-BH occurring in the database in Sect. 3. We also make the CMC database representative for the Milky Way GC system, by applying weights to the result of GCs with different N by a factor N^{-1} , such that the logarithmically spaced N values represent an initial GC mass function of the form M_0^{-2} . We then only consider the low metallicity models ($Z = 2 \times 10^{-4}$ and $Z = 2 \times 10^{-3}$), with relative weights 4:1, representative for the Milky Way GC population (e.g., Harris 1996).

We only consider *hard* binaries (Heggie 1975), defined as those whose absolute value of the binding energy is greater than the average kinetic energy of particles in the GC core. This is done to exclude loosely bound pairs that are constantly being assembled and destroyed.

As clusters evolve they lose mass and stars due to internal two-body relaxation and interactions with the Galactic tidal field. Therefore, they dissolve over a period which depends on the cluster relaxation time scale and their position within the Galactic potential. In our models, clusters are assumed to be completely *dissolved* once $t_{\text{rlx}} > M_{\text{SC}}/\dot{M}_{\text{SC}}$ where t_{rlx} and M_{SC}

indicate the relaxation time and the total mass of the clusters, respectively (Kremer et al. 2020).

3. Origin of *Gaia* BH3-like binaries

In this section, we explore the formation of S-BH binaries in the CMC catalogue that are the most similar to *Gaia* BH3. From the 1837 S-BH binaries in the catalogue, we filter out 565 binaries that are accreting. The remaining 1435 detached binaries are shown in Fig. 1, where the contribution of each of the models is weighted as explained in Sec. 2. From these binaries, 78% are ejected and the rest remain in the cluster, either until it dissolves or the simulation ends. We assume that S-BH binaries that survive until 13 Gyr in non-dissolved clusters will remain in the cluster until dissolution, which is justified by the decreasing velocity dispersion of the cluster, making it less likely to break up the binary in its final stages.

From the sample of detached binaries, we select those most similar to *Gaia* BH3, which we define as those whose parameters all fall within the red dashed lines in the subplots of Fig. 1. The red lines span the following ranges: $m_{\text{BH}} \in [25, 45] M_{\odot}$, $m_{\star} \in [0.2, 1] M_{\odot}$, $P \in [400, 40000]$ d, and $e \in [0.63, 0.83] M_{\odot}$. These ranges are much larger than the typical uncertainties on the observationally inferred parameters of *Gaia* BH3 – which are of order 1-2% – and are chosen to (i) cover a roughly similar fraction of the ranges of the parameters found in the models and (ii) end up with a reasonable number of S-BH.

This criteria selects nine binaries. Next we refine this sample to match the model GC properties with what we know of the ED-2 stream, but before we do that, it is interesting to note that *Gaia* BH3-like binaries exist and that all of them have a dynamical origin.

From the nine resembling S-BH binaries, we narrow down our sample by selecting only those binaries that are ejected at very late times or remain in the cluster until dissolution. We note that there are no escapers (of these nine) after the first ~ 500 Myr. This filtering is done because early escapers drift away from the cluster. For the orbit of ED-2, escapers have an average drift velocity with respect to the progenitor cluster of ~ 1 km/s (e.g., Küpper et al. 2010; Roberts et al. 2024), such that escapers in the first few Gyr of the cluster’s life would no longer be associated with the stream, which contains stars that were lost in the final ~ 3 Gyr of the cluster’s life (Erkal et al. 2017; Gieles et al. 2021).

Two out of the nine binaries in our sample pass this further criteria. We refer to these two candidate *Gaia* BH3-like binaries as cSBH1 and cSBH2. For cSBH1 (cSBH2), the masses of the components are $m_{\text{BH}} = 29.9$ (40.5) M_{\odot} and $m_{\star} = 0.21$ (0.44) M_{\odot} . The semimajor axis is $a = 69$ (57) AU – which implies a period of $P = 37760$ (24791) d – and the eccentricity is $e = 0.72$ (0.80). Both binaries originate from the cluster model with initial parameters $N = 2 \times 10^5$, $r_v = 4$ pc. The initial mass for this model is $M_0 = 1.2 \times 10^5 M_{\odot}$, which is the lowest mass GC in the CMC catalogue. This is within a factor of a few of the mass estimate provided by Balbinot et al. (2024) derived by the light elements spreads. Combined with the upper limits from the abundances and dissolution time (Sect. 1), we therefore conclude that the models prefer an initial GC mass $\lesssim 10^5 M_{\odot}$.

Both of these binaries form dynamically roughly 100 Myr after GC formation, corresponding to the moment of core collapse of the BH subsystem. The classic picture is that a binary forms in a three-body interaction (Heggie 1975; Atallah et al. 2024). We note that the outcome of core collapse is the production of a dynamically active BBH, likely involving $\sim 5 - 10$ particles

² Additional BH candidates are observed in GCs as accreting sources via their X-ray/radio emission (e.g., Maccarone et al. 2007; Strader et al. 2012; Miller-Jones et al. 2015).

³ For the initial density profile of these models $r_v \approx 1.25 r_h$, where r_h is the half-mass radius.

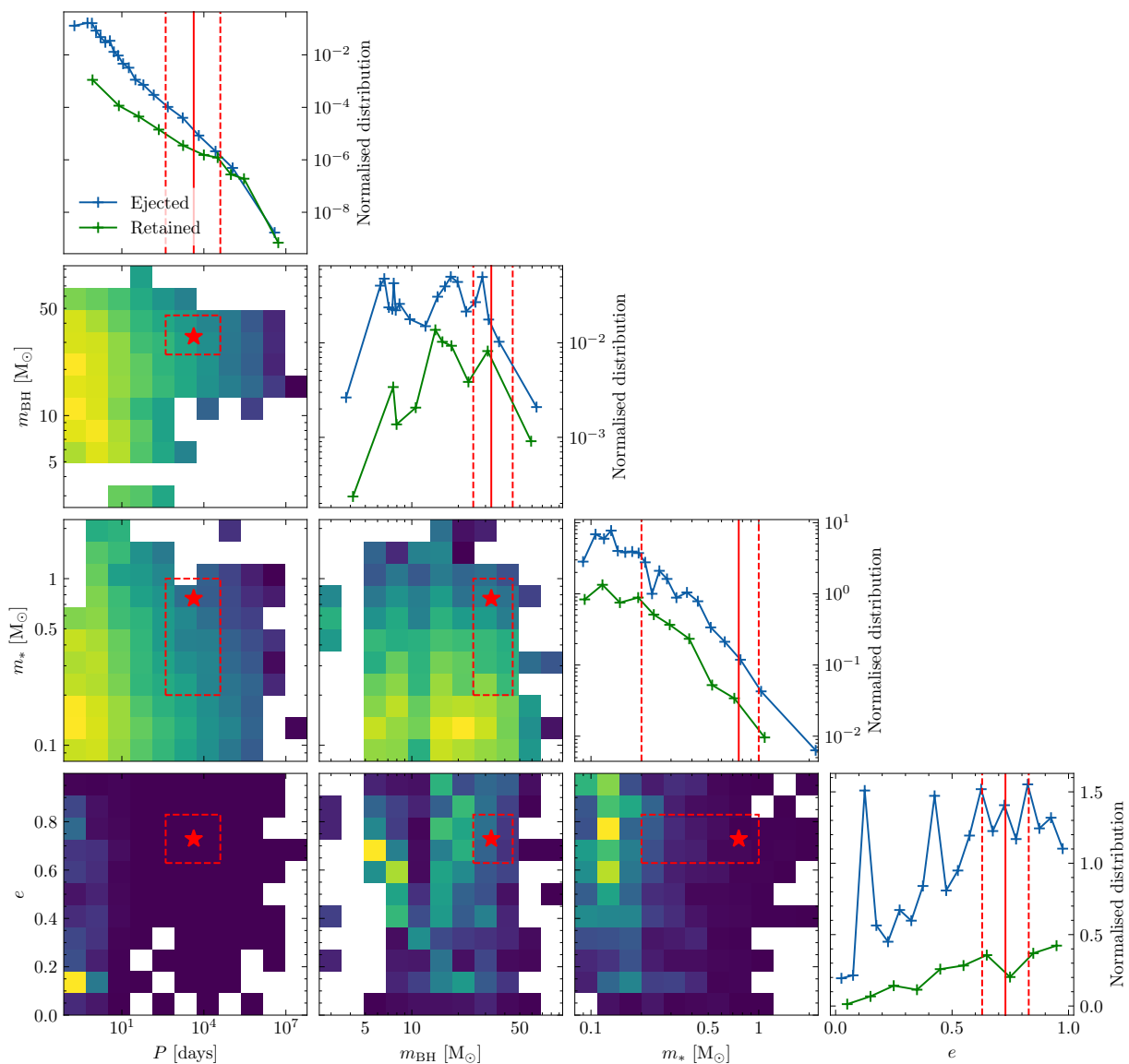


Fig. 1: Probability distribution functions for the masses of the BH and star (m_{BH} and m_* , respectively) and orbital parameters (period P and eccentricity e) for all the detached S-BH binaries in the cluster simulations of Kremer et al. (2020). For ejected binaries, we show their parameters at the time of ejection. The contribution of each binary to the histogram is weighted as explained in Sec. 2. In red (continuous line for 1D histograms, star symbol for 2D histograms), the values for *Gaia* BH3. In dashed red line, the range for the analysis of *Gaia* BH3-like binaries in Sec. 3. The green lines in the 1D histogram include only the S-BH binaries that are not ejected from their parent cluster.

(Tanikawa et al. 2012). The S-BH appears to form in an intermediate step, involving two stars and a BH, and it seems to be a by-product of BBH formation. Developing a full understanding of the relation between the formation of the S-BH and the BBH is beyond the scope of this work. We here simply note it as a curiosity worth looking into in future work, and in Sect. 4.3 we discuss the implications.

In the case of cSBH1, it is directly formed in a three-body interaction, whereas cSBH2 is the exchange of two three-body binaries. Both S-BH systems remain in the cluster until it dissolves. After formation, these binaries undergo 18 and 7 strong interactions respectively, implying that even if formed from binary evolution, dynamical interactions in the ED-2 progenitor need to be included to understand their final properties.

If we do not exclude early escapers from our sample (i.e., if we consider the nine non-accreting binaries whose param-

eters all fall within the red boxes in Fig. 1), we find a similar interaction history. Except for cSBH1, all nine S-BH binaries are formed via three-body encounters. The ejected binaries undergo multiple strong interactions (ranging from one to twelve) until they escape the cluster. From these, all but one are ejected following interactions with BBHs. A high rate of binary-binary interactions is expected in clusters with relatively low number of BHs (Marín Pina & Gieles 2024).

4. Implications

4.1. Formation efficiency

To make the result more quantitative, we now extend our analysis to compute how many S-BH binaries are expected to be ejected in the ED-2 stream. We begin by defining the forma-

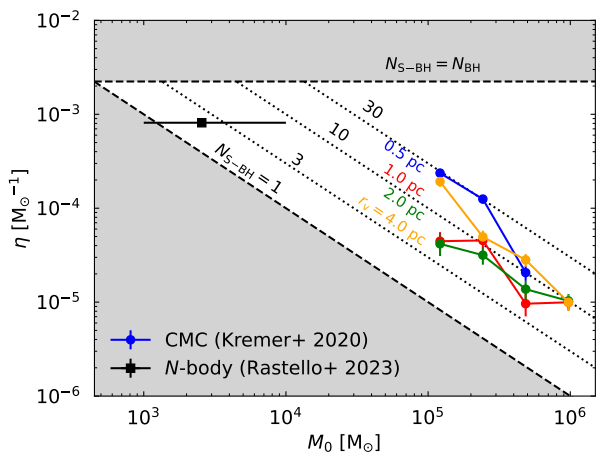


Fig. 2: Formation efficiency of S-BH in all CMC models with $Z = 2 \times 10^{-4}$ (bullets) and all S-BH formed in the N -body results of Rastello et al. (2023) for Solar metallicity (square). Dashed lines show the maximum η , corresponding to all BHs in the cluster being in an S-BH and the minimum η corresponding to clusters with one BH. The dotted lines correspond to constant numbers of S-BH.

tion efficiency, η , as the number of ejected S-BH binaries in our model per unit of initial cluster mass (M_0). In the CMC models, we find a clear dependence of η on the initial cluster mass and virial radius, shown in Fig. 2. The formation efficiency is higher in denser and less massive clusters; however, this trend does not extend to lower masses ($\lesssim 10^4 M_\odot$). There, it levels off, as there is a hard limit where the number of ejected S-BH binaries, N_{S-BH} , equals the initial number of BHs in the cluster, N_{BH} . For more massive clusters, formation of S-BH binaries is relatively inhibited by pronounced dynamical heating from their large central BH populations (Kremer et al. 2018a).

In the CMC regime, the formation efficiency can be approximated by the following power law:

$$\eta = 1.6 \times 10^{-4} M_\odot^{-1} \left(\frac{M_0}{10^5 M_\odot} \right)^{-1.2} \left(\frac{r_v}{1 \text{ pc}} \right)^{-0.42}. \quad (1)$$

Extrapolating to the mass estimate for the ED-2 progenitor ($5 \times 10^4 M_\odot$, Sect. 1) and $r_v = 2 - 4$ pc, implies that the ED-2 stream contains about $\sim 9 - 13$ S-BH binaries, of which $\sim 2 - 3$ are retained in the cluster. We conclude that dynamical formation of *Gaia* BH3 is a viable explanation for its origin.

4.2. Number of S-BH in the Galactic halo

With the relation $\eta(M_0, r_v)$ from equation (1) we can estimate the total number of S-BH binaries produced dynamically in the complete population of Galactic GCs. We write the initial GC mass function (GCMF) as $\psi_0(M_0) = AM_0^{-2}$. We then assume that all clusters lose 40% of their mass by stellar evolution and an amount $\Delta \approx 2 \times 10^5 M_\odot$ by evaporation. This amount is required to get the turn-over mass in the GCMF at $\sim 2 \times 10^5 M_\odot$ if mass is lost at a constant rate (Jordán et al. 2007). The evolved GCMF can then be written as

$$\psi(M) = \mu_{\text{sev}} A (M + \Delta)^{-2}, \quad (2)$$

where $\mu_{\text{sev}} \approx 0.6$. The normalisation constant A is found from the total number of Milky Way GCs (157) and integrating $\psi(M)$

from $10^2 M_\odot$ (roughly the lowest mass Milky Way GC) to $10^6 M_\odot$.

The total number of S-BH binaries produced by all Milky Way GCs, including the dissolved ones, is then

$$N_{S-BH} = \int_{10^4 M_\odot}^{10^6 M_\odot} \eta(M_0, r_v) M_0 \psi_0(M_0) dM_0, \quad (3)$$

$$\approx 10^5. \quad (4)$$

Here we weighed the results for different r_v equally. We note that there are no CMC models in the range $10^4 \leq M_0/M_\odot \leq 10^5$, so the results depends on an extrapolation outside of the range of the CMC grid. From the models of lower mass clusters of Rastello et al. (2023) (Fig. 2), this seems reasonable for $r_v \geq 1$ pc.

Because most S-BH are produced by low-mass dissolved GCs, the number density of S-BH in the Galactic halo follows the initial density distribution of GCs in the Milky Way: $n_{GC} \propto R_G^{-4.5}$ between 1 kpc and 100 kpc (e.g. Fall & Zhang 2001; Gieles & Gnedin 2023). Scaling this to a total number of 10^5 , we then find that at the solar radius the number density of S-BH in the halo is $n_{S-BH} \approx 1 \text{ kpc}^{-3}$, corresponding to ~ 1 within the distance to *Gaia* BH3. Within a distance of 1 – 3 kpc from the Sun there are 5 – 130 S-BH expected from (dissolved) GCs.

4.3. Connecting to gravitational wave sources

As the catalogue of BBH mergers detected via gravitational waves by LIGO/Virgo/KAGRA (LVK) grows (Abbott et al. 2023), the details of the astrophysical origin of these sources remain elusive. Dynamical formation within GCs has emerged as one possible scenario and has been studied at length using N -body cluster simulations including CMC (e.g., Rodriguez et al. 2016). In GCs, the dynamical formation of S-BH binaries like *Gaia* BH3 and the three BH candidates observed in NGC 3201 is an inevitable byproduct of the same processes that lead to formation of merging BH pairs (e.g., Kremer et al. 2018b). Thus, detection of sources like *Gaia* BH3 provide important constraints on the properties of BHs in clusters, their dynamics, and the role of GCs in forming GW sources.

In Fig. 3, we show the cumulative distribution of BH masses from our CMC models for BHs undergoing BH mergers (gray) and BHs found in S-BH binaries (blue; including both retained and ejected binaries), again adopting the cluster weighting scheme from Section 2. For reference, we also show distributions of known stellar-mass BHs with mass measurements: low- and high-mass X-ray binaries (red curve) taken from (Remillard & McClintock 2006; Corral-Santana et al. 2016), BH mergers (black curve) from GWTC-3 (Abbott et al. 2023), and the three *Gaia* BH3 binaries⁴. As shown, GCs naturally produce dynamically-active populations of BHs with masses consistent with both the LVK sources and *Gaia* BH3. Future detections of more S-BH binaries in the Milky Way will provide further constraints on the potential connection between these populations.

⁴ We note that the X-ray binary and GW histograms shown in Fig. 3 are raw data and do not take into account detection biases or astrophysical weighing (for discussion, see Fishbach & Kalogera 2022).

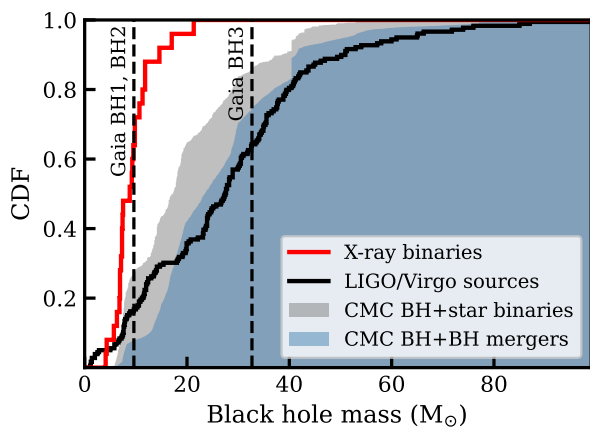


Fig. 3: Cumulative distribution of measured BH masses observed as X-ray binaries (Remillard & McClintock 2006; Corral-Santana et al. 2016) and as GW sources (Abbott et al. 2023) compared to distributions of BH masses identified in our CMC models. Vertical dashed lines show measured masses for the three *Gaia* BHs.

5. Discussion

5.1. Binary fraction

The prediction of the number of S-BH might be a lower limit due to the relatively low primordial binary fraction in the CMC models (5%). For solar-type stars the initial binary/multiplicity fraction could be 30-40% (Moe & Di Stefano 2017) and for massive stars it is close to 100% (Sana et al. 2012). A higher binary fraction leads to higher rate of binary-binary interactions providing an additional pathway to formation of S-BH in exchange interactions (e.g., González et al. 2021; Tanikawa et al. 2024).

5.2. Stellar masses

The stellar masses in the overall population of S-BH in the CMC models peaks at relatively low masses ($\sim 0.2 M_{\odot}$), which makes the majority of these S-BH difficult to detect. Recent analysis of the stellar mass function Milky Way GCs (Baumgardt et al. 2023; Dickson et al. 2023) suggests that the low-mass end of the mass function could be flatter than what is assumed in CMC. This would lead to higher stellar masses in S-BH binaries. Estimating this effect requires additional dynamical modelling and is beyond the scope of this work, however see Weatherford et al. (2021) for preliminary efforts.

6. Conclusions

Gaia BH3 belongs to the ED-2 stream, so its kinematics suggests that it was formed in the ED-2 progenitor GC. In this Letter, we studied the dynamical formation and ejection of *Gaia* BH3-like binaries in GCs. We analysed the public catalogue of star-by-star GC simulations in Kremer et al. (2020), and compared it to *Gaia* BH3. We found that the properties of *Gaia* BH3 – masses, period, eccentricity and lack of chemical pollution – are compatible with it being assembled dynamically from a previously unbound star and a BH that had not undergone joint stellar evolution.

Furthermore, we extend our analysis to the whole ED-2 stream in particular and the Galactic halo in general. We predict

that the stream contains of the order of $\sim 9 - 13$ dynamically-assembled S-BH binaries, whereas the halo contains $\sim 10^5$.

Acknowledgements. The authors thank Eduardo Balbinot for discussions on ED-2 and the *Gaia* group at ICCUB for useful interactions. DMP and MG acknowledge financial support from the grants PID2021-125485NB-C22, EUR2020-112157, CEX2019-000918-M funded by MCIN/AEI/10.13039/501100011033 (State Agency for Research of the Spanish Ministry of Science and Innovation) and SGR-2021-01069 (AGAUR). SR acknowledges support from the Beatrú de Pinós postdoctoral program under the Ministry of Research and Universities of the Government of Catalonia (Grant Reference No. 2021 BP 00213). Support for KK was provided by NASA through the NASA Hubble Fellowship grant HST-HF2-51510 awarded by the Space Telescope Science Institute, which is operated by the Association of Universities for Research in Astronomy, Inc., for NASA, under contract NAS5-26555.

References

- Abbott, R., Abbott, T. D., Acernese, F., et al. 2023, *Physical Review X*, 13, 041039
- Antonini, F., Gieles, M., Dosopoulou, F., & Chattopadhyay, D. 2023, *MNRAS*, 522, 466
- Arca Sedda, M., Kamlah, A. W. H., Spurzem, R., et al. 2024, *MNRAS*, 528, 5119
- Askar, A., Szkudlarek, M., Gondek-Rosińska, D., Giersz, M., & Bulik, T. 2017, *MNRAS*, 464, L36
- Atallah, D., Weatherford, N. C., Trani, A. A., & Rasio, F. 2024 [arXiv:2402.12429]
- Balbinot, E., Dodd, E., Matsuno, T., et al. 2024 [arXiv:2404.11604]
- Balbinot, E., Helmi, A., Callingham, T., et al. 2023, *A&A*, 678, A115
- Baumgardt, H., Hénauld-Brunet, V., Dickson, N., & Sollima, A. 2023, *MNRAS*, 521, 3991
- Corral-Santana, J. M., Casares, J., Muñoz-Darias, T., et al. 2016, *A&A*, 587, A61
- Di Carlo, U. N., Agrawal, P., Rodríguez, C. L., & Breivik, K. 2024, *ApJ*, 965, 22
- Dickson, N., Hénauld-Brunet, V., Baumgardt, H., Gieles, M., & Smith, P. J. 2023, *MNRAS*, 522, 5320
- Dodd, E., Callingham, T. M., Helmi, A., et al. 2023, *A&A*, 670, L2
- El-Badry, K., Rix, H.-W., Cendes, Y., et al. 2023a, *MNRAS*, 521, 4323
- El-Badry, K., Rix, H.-W., Quataert, E., et al. 2023b, *MNRAS*, 518, 1057
- Erkal, D., Kozlov, S. E., & Belokurov, V. 2017, *MNRAS*, 470, 60
- Fall, S. M. & Zhang, Q. 2001, *ApJ*, 561, 751
- Fishbach, M. & Kalogera, V. 2022, *ApJ*, 929, L26
- Gaia* Collaboration, E. e. a. 2024, 58
- Gieles, M., Erkal, D., Antonini, F., Balbinot, E., & Peñarrubia, J. 2021, *Nature Astronomy*, 5, 957
- Gieles, M. & Gnedin, O. Y. 2023, *MNRAS*, 522, 5340
- Giesers, B., Dreizler, S., Husser, T.-O., et al. 2018, *MNRAS*, 475, L15
- Giesers, B., Kamann, S., Dreizler, S., et al. 2019, *A&A*, 632, A3
- González, E., Kremer, K., Chatterjee, S., et al. 2021, *ApJ*, 908, L29
- Harris, W. E. 1996, *AJ*, 112, 1487
- Heggie, D. C. 1975, *MNRAS*, 173, 729
- Jordán, A., McLaughlin, D. E., Côté, P., et al. 2007, *ApJS*, 171, 101
- Kotko, I., Banerjee, S., & Belczynski, K. 2024 [arXiv:2403.13579]
- Kremer, K., Chatterjee, S., Rodríguez, C. L., & Rasio, F. A. 2018a, *ApJ*, 852, 29
- Kremer, K., Ye, C. S., Chatterjee, S., Rodríguez, C. L., & Rasio, F. A. 2018b, *ApJ*, 855, L15
- Kremer, K., Ye, C. S., Rui, N. Z., et al. 2020, *ApJS*, 247, 48
- Küpper, A. H. W., Kroupa, P., Baumgardt, H., & Heggie, D. C. 2010, *MNRAS*, 401, 105
- Maccarone, T. J., Kundu, A., Zepf, S. E., & Rhode, K. L. 2007, *Nature*, 445, 183
- Marín Pina, D. & Gieles, M. 2024, *MNRAS*, 527, 8369
- Miller-Jones, J. C. A., Strader, J., Heinke, C. O., et al. 2015, *MNRAS*, 453, 3918
- Moe, M. & Di Stefano, R. 2017, *ApJS*, 230, 15
- Portegies Zwart, S. F. & McMillan, S. L. W. 2000, *ApJ*, 528, L17
- Rastello, S., Iorio, G., Mapelli, M., et al. 2023, *MNRAS*, 526, 740
- Remillard, R. A. & McClintock, J. E. 2006, *ARA&A*, 44, 49
- Roberts, D., Gieles, M., Erkal, D., & Sanders, J. L. 2024 [arXiv:2402.06393]
- Rodríguez, C. L., Weatherford, N. C., Coughlin, S. C., et al. 2022, *ApJS*, 258, 22
- Rodríguez, C. L., Zevin, M., Pankow, C., Kalogera, V., & Rasio, F. A. 2016, *ApJ*, 832, L2
- Sana, H., de Mink, S. E., de Koter, A., et al. 2012, *Science*, 337, 444
- Strader, J., Chomiuk, L., Maccarone, T. J., Miller-Jones, J. C. A., & Seth, A. C. 2012, *Nature*, 490, 71
- Tanikawa, A., Cary, S., Shikauchi, M., Wang, L., & Fujii, M. S. 2024, *MNRAS*, 527, 4031
- Tanikawa, A., Hut, P., & Makino, J. 2012, *New A*, 17, 272
- Weatherford, N. C., Fragione, G., Kremer, K., et al. 2021, *ApJ*, 907, L25
- Weatherford, N. C., Kiroğlu, F., Fragione, G., et al. 2023, *ApJ*, 946, 104